INSTITUTE OF PHYSICS PUBLISHING MODELLING AND SIMULATION IN MATERIALS SCIENCE AND ENGINEERING

Modelling Simul. Mater. Sci. Eng. **13** (2005) 329–340 doi:10.1088/0965-0393/13/3/003

An analytical model for the effect of elastic modulus mismatch on laminate threshold strength

Alok Paranjpye, Glenn E Beltz and Noel C MacDonald

Department of Mechanical and Environmental Engineering, University of California, Santa Barbara, CA 93106-5070, USA

E-mail: alokp@engineering.ucsb.edu

Received 25 May 2004, in final form 28 January 2005
Published 9 March 2005
Online at stacks.iop.org/MSMSE/13/329

Abstract

We present an analytical model for predicting the crack tip stress intensity factor in a laminated composite material with alternating zones of residual biaxial compressive and tensile stresses. Such an arrangement of residual stress zones has been shown to be useful for enhancing the damage tolerance properties of the structure, which are manifested as a 'threshold' strength below which the material cannot fail catastrophically. This model improves upon a previous scheme for predicting crack behaviour in such a material, which assumes homogeneous material properties throughout the laminate. To make the problem tractable, this scheme models the system as a homogeneous anisotropic material when calculating the stress fields at the crack tip arising from tractions applied far away from the crack tip. A comparison of the predictions from both schemes with those from a finite element model of such a system shows that our assumptions yield an improved representation of the material's behaviour. We also present results for optimization of geometrical parameters of the system to obtain the highest possible threshold strength under the limitation of a given set of material properties. We conclude that while this scheme improves upon the homogeneous model, more work is required to predict the stresses at the tip as the crack approaches a material interface before a complete analytical model can be obtained.

1. Introduction

Ceramic materials often present a quandary to the materials designer. They have many properties that are uniquely useful in certain applications, such as high temperature environments, but they bring with them their inherent mechanical unreliability. Colloquially referred to as 'brittle' materials, the strength of ceramics and other similar materials follows statistical distributions (such as Weibull) with a wide distribution of strength values. This

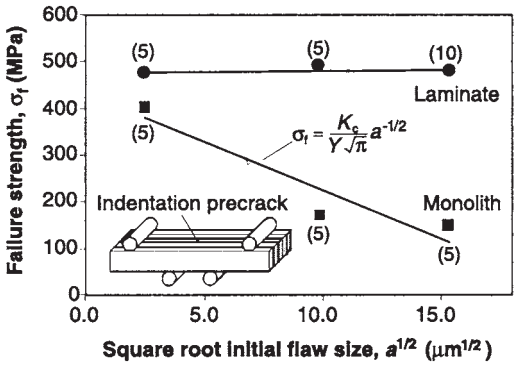

Figure 1. Fracture testing results on an alumina–mullite laminate [1]. The fracture strength is seen to be independent of initial crack size for the composite, but inversely related to crack size for the monolithic ceramic structures. Reprinted with permission from Rao M P *et al* 1999 *Science* **286** 102–5. © 1999 AAAS.

distribution in strength values is due to a synergism of two factors: (i) the lack of plastic flow mechanisms in the crystal structure that are effective for dissipating elastic strain energy, and (ii) the presence of a variety of cracks and similar flaws that locally intensify the stress fields around them, and are inadvertently introduced during the manufacturing process. The size of the largest flaw determines the final strength of the structure.

This phenomenon forces any critical ceramic components in an assembly to be subjected to proof testing prior to service, which adds greatly to the final cost of the solution. Consequently, in the field of ceramics design, a number of mechanisms have been proposed to overcome this drawback. For example, components can be manufactured by consolidating ceramic powders in which the particles have sizes only below a certain value. This limits the size of the largest flaw in the component, making it more reliable against sudden fracture. More recent work [1] has demonstrated that a threshold strength below which failure does not occur can be achieved by introducing layers of regions of compressive stress in the component.

In the experiments by Rao *et al* [1, 2], a composite laminate was formed by fusing together alternate layers of different alumina and mullite fractions, with widths in the range 50 to 600 μm, at high temperature before cooling and testing at room temperature. The differential thermal expansion between the two materials causes residual stresses to build up in the composite, with alternate layers developing biaxial tensile and compressive stresses. The same effect may be obtained from a differential volume change due to a phase transformation, or a chemical reaction. The layered material was pre-cracked prior to testing under different loads and indenters, with the resulting pre-cracks arranged to run perpendicular to the plane direction of the layers. As seen in figure 1, under subsequent tests that loaded these pre-cracks in Mode I, it was found that component strength was independent of the initial crack size. Moreover, a threshold stress did indeed exist, with no failure occurring below a certain stress level. In contrast, similarly treated monolithic ceramic components displayed strength that varied inversely with the pre-crack size.

Similar results were obtained at a different length scale in a silicon–silicon oxide material system [3], with potential application as a robust structural material for micro-electro-mechanical systems (MEMS). Cantilevers made of a composite with alternating layers of Si and SiO_2 with layer widths in the range 1–5 μm were flexed under increasing load until fracture. The control specimens were identically treated and processed cantilevers of single crystal silicon (SCS). The fracture strength was calculated from the end-applied load at fracture. A range of strengths-at-failure was measured in both materials, probably due to processing

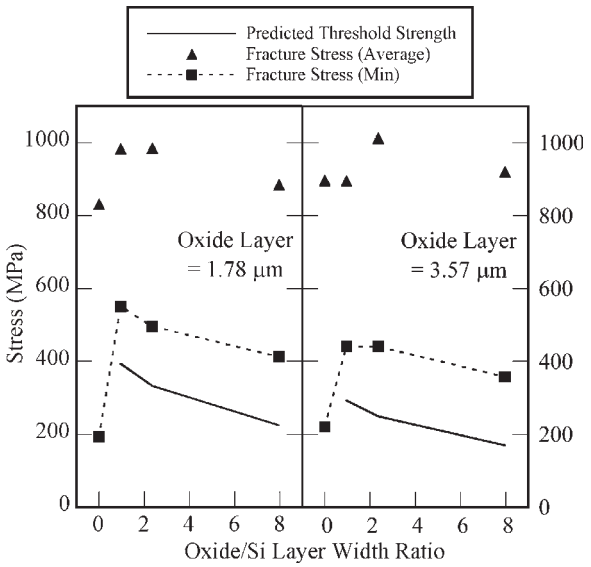

Figure 2. Fracture testing results from [3] for silicon–silicon oxide composites for MEMS applications. The minimum fracture strength for the composites is significantly higher than the minimum fracture strength for the monolithic silicon structures.

induced flaws. However, as shown in figure 2, the lowest fracture strength values for the composite cantilevers were significantly higher than the lowest fracture strength values for the SCS cantilevers, and varied predictably with certain geometric parameters.

1.1. Analytical model for threshold strength

A mathematical model for the threshold strength phenomenon was developed by Rao *et al* [1]. This model assumes compressive layers of thickness t_1 with a residual compressive stress σ_C and tensile layers of thickness t_2 with a tensile stress σ_T. The biaxial residual stresses in the layers are given [4] by

$$\begin{aligned} \sigma_C &= \varepsilon E_1' \left(1 + \frac{t_1 E_1'}{t_2 E_2'}\right)^{-1}, \\ \sigma_T &= -\sigma_C \frac{t_1}{t_2}, \end{aligned} \tag{1}$$

where $\varepsilon \equiv \Delta\alpha \Delta T$. The parameter $\Delta\alpha$ is the differential in the coefficients of thermal expansion of the two materials and ΔT is the temperature difference between testing (or service) temperature and a temperature where the thermal residual stresses are zero. $E_i' = E_i/(1 - \nu_i)$ is an effective Young's modulus, derived from the actual Young's modulus E_i and Poisson's ratio ν_i of materials 1 (compressive layer) and 2 (tensile layer). The model further assumes a crack spanning a tensile layer and just extending into the two compressive layers on either side, as well as a tensile load applied parallel to the layers and perpendicular to the crack, as shown in figure 3.

The analysis yields a stress intensity factor at the crack tip for this stress field, albeit under the important assumption of an elastically homogeneous system. The expression obtained for a crack of length $2a$ is given by

$$K = \sigma_a \sqrt{\pi a} + \sigma_c \sqrt{\pi a} \left[\left(1 + \frac{t_1}{t_2}\right) \frac{2}{\pi} \sin^{-1} \left(\frac{t_2}{2a}\right) - 1 \right]. \tag{2}$$

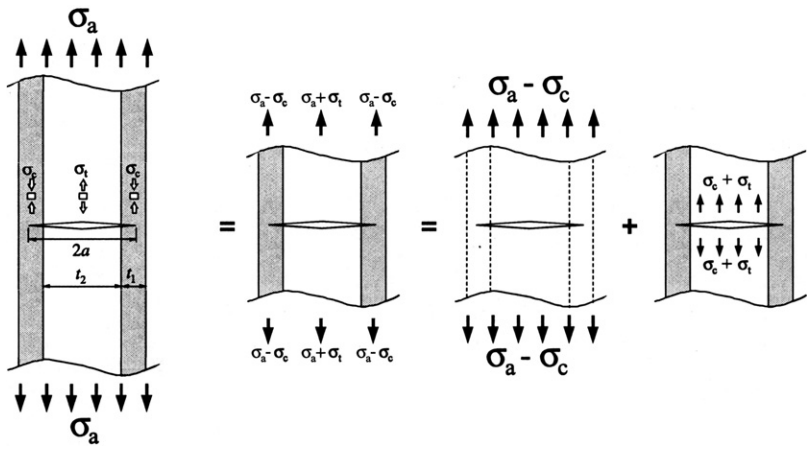

Figure 3. A schematic of the crack geometry and residual and applied stresses assumed in the mathematical modelling. The crack is assumed to just extend into the compressive layers. The stress superposition scheme used to obtain the crack tip stress intensity factor is also indicated here.

Equation (2) shows that the stress intensity factor at the crack tip is lowered as a larger fraction of the crack length lies in the two compressive layers on either side of the tensile layer. This implies that the applied stress required for extending the crack increases as the crack penetrates further into the compressive layers. Therefore, the threshold strength is the applied stress required to extend the crack as the crack length just spans a tensile layer and the two compressive layers on either side. Setting $2a = t_2 + 2t_1$ and $K = K_C$ of the compressive layer material, the threshold strength is given by

$$\sigma_{thr} = \frac{K_c}{\sqrt{\pi(t_2/2)\,(1 + 2t_1/t_2)}} + \sigma_c \left[1 - \left(1 + \frac{t_1}{t_2}\right)\frac{2}{\pi}\sin^{-1}\left(\frac{t_2}{t_2 + 2t_1}\right)\right]. \tag{3}$$

To further validate this result, it has also been shown [5] that the value of threshold stress for a crack initially restricted to the tensile layer is lower than its value when the crack extends into the compressive layers. The same workers also showed that the highest possible threshold stresses for a given material system could be obtained by minimizing the thickness of the layers and by optimizing the layer thickness ratio. They showed that the optimal threshold strength for low toughness materials of approximately $0.3\varepsilon E_1'$ may be obtained by keeping the tensile–compressive layer thickness ratio in the range 1–2.8.

The major limitation of the theoretical analysis so far lies in the assumption of homogeneous elastic properties for the system of two materials. As such, all predictions made from these equations are limited in their accuracy when the Young's modulus and Poisson's ratio values of the two materials in the laminate are significantly different. Hbaieb and McMeeking [6] conducted a finite element simulation of this geometry, and presented extensive results on the variation of threshold stress with material modulus ratios. A comparison of the results obtained from the finite element simulations and the homogeneous model shows the results varying significantly as the material modulus ratio changes. As new material systems are employed in this composite geometry, there is also a need to accurately optimize the layer thickness ratio to achieve the highest possible threshold strength under the limitations of inherent material properties, and technological limitations on minimum layer thickness. Using finite element simulations to optimize the layer thickness ratio is a cumbersome process; involving constructing many models with different layer thickness ratios. Consequently,

we felt a need existed for an analytical model for the threshold strength in this system that could incorporate the effects of different elastic properties for the two component materials in the composite. This paper is an attempt to obtain a more accurate analytical representation of the threshold stress phenomenon.

2. An orthotropic laminate

To arrive at an alternate analytical expression for the stress intensity factor at the crack tip, we treat the bimaterial laminate as an anisotropic material in a limited sense. We assume that the stresses building up at the crack tip due to loads applied at the material boundary are similar in our composite as they would be for a crack tip of identical geometry in an *anisotropic* material. Tada *et al* [7] give an expression relating the energy release rate at the crack tip in an anisotropic material to the stress intensity factor K_i for the corresponding isotropic boundary value problem

$$G_i = \boldsymbol{C} K_i^2 \Rightarrow G_i^{\text{anisotropic}} = \boldsymbol{C}(K_i^{\text{isotropic}})^2, \tag{4}$$

where $\boldsymbol{C}$ is computed from the elements of the compliance matrix for the anisotropic material. The stress intensity factor for the isotropic boundary value problem is identical to that evaluated under the assumption of homogeneous elastic properties [1], which takes into account the effect of the residual stresses on the crack tip stress intensity, and which we will refer to as $K_1^{\text{isotropic}}$. For the case of a bimaterial laminate, the material is orthotropic (specifically, transversely isotropic), and for a crack opening in Mode 1, $\boldsymbol{C}$ is given by

$$\boldsymbol{C} = \sqrt{\frac{A_{11}A_{22}}{2}}\left[\sqrt{\frac{A_{22}}{A_{11}}} + \frac{2A_{12} + A_{66}}{2A_{11}}\right]^{1/2}, \tag{5}$$

where the A_{ij}s are the elements of the compliance matrix. The energy release rate thus obtained can be related back to a crack tip stress intensity factor in an anisotropic material as

$$K_1^{\text{anisotropic}} = \sqrt{\frac{E_1}{1-\nu_1^2}}(G_1^{\text{anisotropic}})^{1/2} \tag{6}$$

for the plane strain situation we will consider. The Young's modulus and Poisson's ratio in (6) are for the material at the crack tip, which in our case is the compressive layer material. From (4) and (6), we obtain a factor F relating the crack tip stress intensity in an anisotropic material to the stress intensity at the tip of an identical crack in an isotropic material.

$$\boldsymbol{F} = \frac{K_1^{\text{anisotropic}}}{K_1^{\text{isotropic}}} = \sqrt{\frac{E_1 \boldsymbol{C}}{1-\nu_1^2}}. \tag{7}$$

2.1. Constitutive relations for an orthotropic laminate

To obtain the compliance matrix for an orthotropic laminate with transverse isotropy in the 2–3 plane, we solve the general elasticity problem as shown in figure 4. We apply stresses along the material axes of isotropy and compute the resultant strains. The ratio of the strains to the stresses gives the elements of the elasticity matrix, related to the material constants of the individual components of the laminate and their relative thickness. For a transversely isotropic

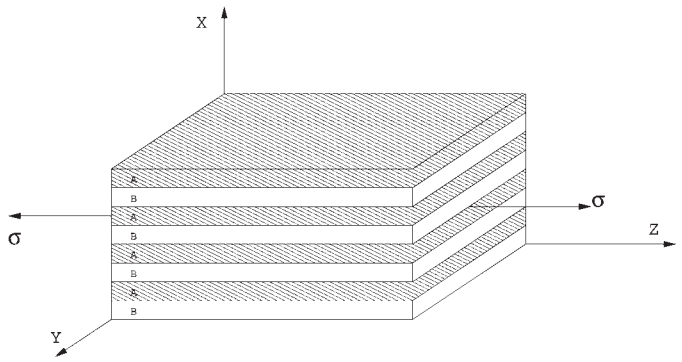

Figure 4. A schematic of the bimaterial laminate geometry; 2–3 is the plane of transverse isotropy for this model. The elastic problem is solved for a uniform stress applied one by one along the x, y, and z axes to obtain the compliance matrix.

material there are only five independent elastic constants, and the compliance matrix is

$$\begin{bmatrix} A_{11} & A_{12} & A_{13} & 0 & 0 & 0 \\ A_{21} & A_{22} & A_{23} & 0 & 0 & 0 \\ A_{31} & A_{32} & A_{33} & 0 & 0 & 0 \\ 0 & 0 & 0 & A_{44} & 0 & 0 \\ 0 & 0 & 0 & 0 & A_{55} & 0 \\ 0 & 0 & 0 & 0 & 0 & A_{66} \end{bmatrix} = \begin{bmatrix} S_{11} & S_{12} & S_{12} & 0 & 0 & 0 \\ S_{12} & S_{22} & S_{23} & 0 & 0 & 0 \\ S_{12} & S_{23} & S_{22} & 0 & 0 & 0 \\ 0 & 0 & 0 & 2(S_{22}-S_{23}) & 0 & 0 \\ 0 & 0 & 0 & 0 & S_{66} & 0 \\ 0 & 0 & 0 & 0 & 0 & S_{66} \end{bmatrix}, \tag{8}$$

where

$$S_{11} = \frac{E_B^2 t_A t_B (1-\nu_A-2\nu_A^2)+E_A E_B (t_B^2(1-\nu_A)+t_A^2(1-\nu_B)+4t_A t_B \nu_A \nu_B)+E_A^2 t_A t_B (1-\nu_B-2\nu_B^2)}{E_A E_B (t_A+t_B)[E_B t_B (1-\nu_A)+E_A t_A (1-\nu_B)]}, \tag{9}$$

$$S_{12} = \frac{t_A \nu_A (1-\nu_B)+t_B \nu_B (1-\nu_A)}{E_B t_B (1-\nu_A)+E_A t_A (1-\nu_B)}, \tag{10}$$

$$S_{23} = \frac{(t_A+t_B)[E_B t_B \nu_B (1-\nu_A^2)+E_A t_A \nu_A (1-\nu_B^2)]}{E_B^2 t_B^2 (1-\nu_A^2)+2E_A E_B t_A t_B (1-\nu_A \nu_B)+E_A^2 t_A^2 (1-\nu_B^2)}, \tag{11}$$

$$S_{22} = \frac{(t_A+t_B)[E_B t_B (1-\nu_A^2)+E_A t_A (1-\nu_B^2)]}{E_B^2 t_B^2 (1-\nu_A^2)+2E_A E_B t_A t_B (1-\nu_A \nu_B)+E_A^2 t_A^2 (1-\nu_B^2)}, \tag{12}$$

$$S_{44} = 2(S_{22}-S_{23}) = \frac{2(t_A+t_B)(1-\nu_A)1-\nu_B)}{E_B t_B (1+\nu_A)+E_A t_A (1+\nu_B)}, \tag{13}$$

$$S_{66} = \frac{E_B t_A (1+\nu_A)+E_A t_B (1+\nu_B)}{E_A E_B (t_A+t_B)}. \tag{14}$$

The factor $\boldsymbol{F}$, relating $K_1^{\text{anisotropic}}$ to $K_1^{\text{isotropic}}$, is calculated using (9)–(14). The expression is cumbersome, does not in itself offer any new insights and is consequently not presented explicitly here. However, it is amenable to analysis and manipulation using symbolic algebra software, and has been verified to be equal to unity when the condition $E_A = E_B$ and $\nu_A = \nu_B$ is applied. The expression for crack tip stress intensity is therefore given by

$$K^{\text{anisotropic}} = \sqrt{\frac{E_1 \boldsymbol{C}}{1-\nu_1^2}} \left[\sigma_a \sqrt{\pi a} + \sigma_c \sqrt{\pi a} \left[\left(1 + \frac{t_1}{t_2} \right) \frac{2}{\pi} \sin^{-1} \left(\frac{t_2}{2a} \right) - 1 \right] \right]. \tag{15}$$

Once again, setting the crack length to span one tensile layer and the compressive layers on either side, we obtain an expression for threshold stress for this model

$$\sigma_{\text{thr}} = \sqrt{\frac{1-\nu_1^2}{E_1 \boldsymbol{C}}} \frac{K_c}{\sqrt{\pi (t_2/2)(1+2t_1/t_2)}} + \sigma_c \left[1 - \left(1 + \frac{t_1}{t_2} \right) \frac{2}{\pi} \sin^{-1} \left(\frac{t_2}{t_2 + 2t_1} \right) \right]. \tag{16}$$

3. Results and discussion

Hbaieb and McMeeking [6] conducted an extensive study on modelling the threshold stress phenomenon in bimaterial laminates using finite element simulations. They compared the results from their finite element model for the crack tip stress intensity as the crack grew into the compressive layers with the predictions from a theoretical model assuming homogeneous elastic properties in each case. The good agreement between the two methods established confidence in their method. Furthermore, they found that their calculations for stress intensities at crack tips near the interfacial boundaries between zones of opposite residual stress matched well with previously well-established theoretical results. They concluded that their finite element predictions were likely to be more accurate than the theoretical model predictions when the two materials in the laminate had non-identical elastic properties.

In order to obtain an estimate of the accuracy of the results obtained from our treatment of a layered composite material as a homogeneous anisotropic material, we compare the results from our model with those obtained previously from the finite element simulations, and from the previous model that assumed homogenous elastic properties. These comparisons are shown in figures 5(*a*) and (*b*) for two layer width ratios. The finite element model results were obtained assuming a Poisson's ratio of 0.32 for both materials, and the same values have been used for obtaining predictions from both analytical models.

We corroborate the results in [6] in that the results from the homogeneous analytical model and the finite element simulations agree very well when identical Young's modulus values are chosen for the two materials. However, as the modulus ratio is increased, and the layer width ratio varies from unity, we can clearly see that the homogeneous model does not provide adequate accuracy of predictions. Our modified analytical model seems to match the finite element results significantly more closely. It is worthwhile to note that our analysis affects only the first term of the original result for threshold strength as seen in equation (16). The first term is independent of any residual stresses in the system, instead reflecting the influence of the critical stress intensity factor of the compressive layer material, and more importantly of the layer width size scale. On a graph of normalized threshold strength versus normalized critical stress intensity, the first term affects only the slope of the line. As we can see in figure 5, the slopes of the result loci for the finite element methods and the anisotropic analytical model match are almost parallel in every case. The y-intercepts of the curves in figures 5(*a*) and (*b*) are

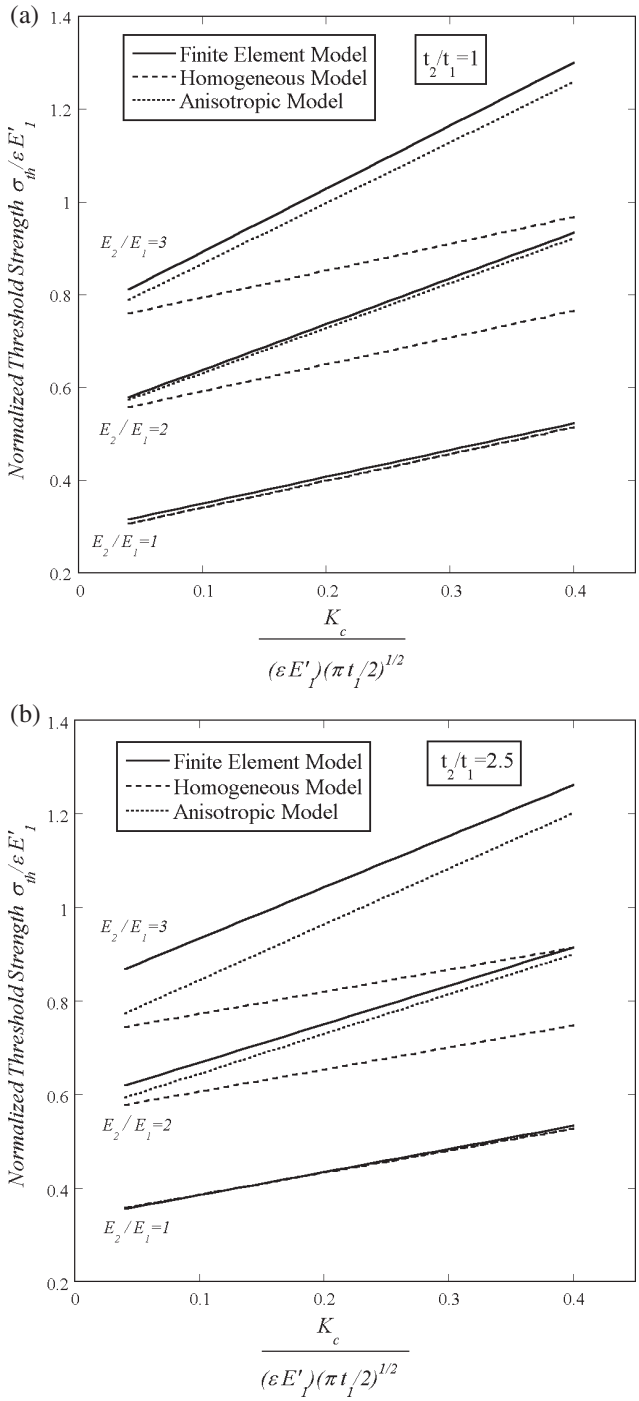

Figure 5. A comparison of the predictions from the homogeneous analytical model, the finite element simulations and the anisotropic model for the threshold strength versus normalized fracture toughness at various ratios of material modulus and layer widths.

not influenced by the modifications to the homogenous model, and lead to an underestimation of the threshold stress at low normalized critical stress intensity.

3.1. Optimization of geometrical parameters

The most important advantage of developing an accurate analytical model for the threshold stress phenomenon in a bimaterial laminate is the ability to optimize the achievable threshold stress for a given set of material properties. Once a material system is chosen, only the geometrical parameters (i) compressive layer thickness and (ii) tensile layer thickness, i.e. the thickness ratio, are controllable to tailor the composite properties. To assist work being conducted on developing a silicon–silicon oxide composite for MEMS applications, we applied our analytical method towards obtaining the highest possible threshold stress in this material system. These composite structures are built using semiconductor processing techniques, and allow very narrow alternating layers to be fabricated. Consequently, the compressive layer widths we investigate lie in the range $2\,\mu$m to 50 nm, and we attempted to find the tensile layer thickness that would give the highest threshold stress. For this system, the composite is 'assembled' at 1200 K and cooled down to room temperature to build up the residual stresses. The silicon layers build up a tensile stress and the oxide layers are left with the corresponding residual compressive stress. The material properties assumed in this calculation are: $E_{\text{Silicon}} = 150\,\text{GPa}$; $\nu_{\text{Silicon}} = 0.25$; $E_{\text{Oxide}} = 90\,\text{GPa}$; $\nu_{\text{Oxide}} = 0.25$; $K_{\text{c}}^{\text{Oxide}} = 0.9\,\text{MPa}\,\text{m}^{1/2}$. The differential strain between the layers is calculated to be 0.189% for our processing temperatures. Figures 6(*a*) and (*b*) show the variation of the threshold stress with the ratio of the tensile layer to compressive layer thickness. The plots show comparisons of the results obtained from the original homogenous model and the modified anisotropic model for compressive layer widths of $2\,\mu$m, $1\,\mu$m, $0.5\,\mu$m, 100 nm and 50 nm. It is significant that as the compressive layer becomes thinner, the homogenous model predicts monotonically increasing threshold stresses as the layer thickness ratio drops. The anisotropic model predicts a well-defined maximum in the threshold stress even for compressive layers approaching the limits of the fabrication process.

It is noteworthy to look at the threshold stresses obtainable in theory, as the compressive layer is made extremely thin. A normalized threshold stress value of 11 corresponds to a threshold stress value of greater than 2 GPa. We can compare these results with the threshold strengths achievable when the size scales employed in [1] ($\sim 500\,\mu$m) are applied. Figure 7 shows the predictions from the two mathematical models when the compressive layers are $500\,\mu$m thick. We see that at larger size scales, the difference between the predictions from the two models is quite small. Moreover, there is almost no difference in the optimized layer width ratio predicted from the two models to achieve the highest possible threshold stress. It also corroborates with the result from [5], that the optimal threshold stress in a homogeneous material system at these layer width scales is close to $0.3\varepsilon E_1$, and is achieved with a layer width ratio in the range 1–2.8.

These modifications applied to the original analytical model address the need for accuracy when two materials of widely varying elastic properties constitute the laminate. However, this model remains only an approximation to an exact formulation for a bimaterial laminate system. The challenge lies in accurately modelling the stresses as the crack tip approaches the interface between a compressive layer and a tensile layer, since it is this situation that ultimately determines the threshold stress. The current model has a shortcoming in not making any allowance for the crack tip approaching an interface, which we believe modifies the stress distributions at the crack tip [8–10] and influences the threshold stress obtainable. We are working on developing an understanding of this situation, and developing a more complete and accurate description of cracking in bimaterial laminates.

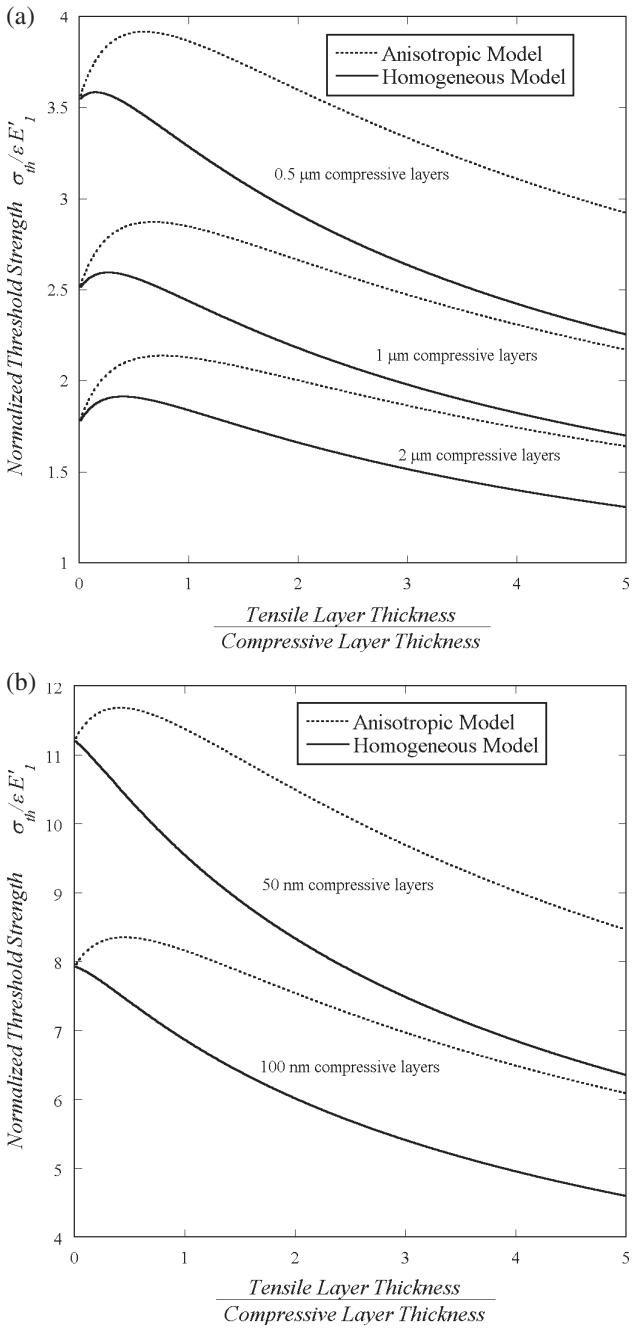

Figure 6. Variation of the normalized threshold strength with layer width ratio at different size scale of layer widths. Comparative results from both analytical models are presented.

4. Conclusions

We have demonstrated a method for modelling the stress distributions around a crack in a layered, inhomogenous composite material by treating it, under certain conditions, as a

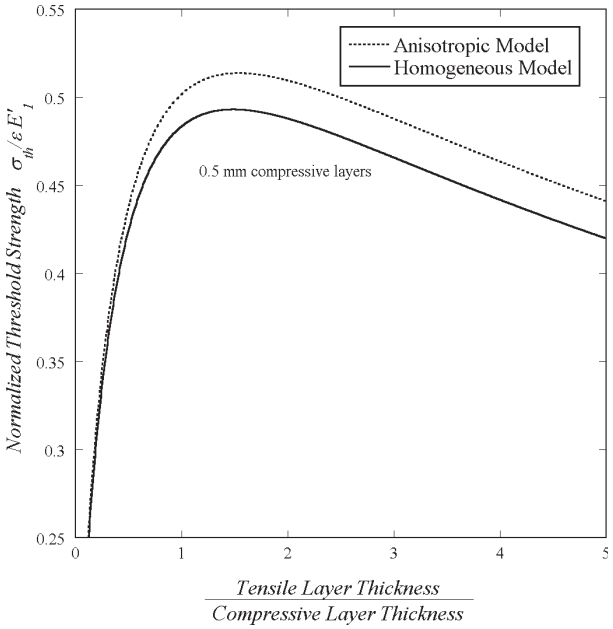

Figure 7. Variation of the normalized threshold strength with layer width ratio at millimetre scale layer widths. Comparative results from both analytical models show little variation at these size scales.

homogenous, anisotropic material. We model the damage tolerance obtained by introducing layers of regions of compressive stress using this approximation scheme. We utilize this scheme to improve upon a previous model for crack behaviour that was inadequate when elastic properties throughout the composite were not uniform. There is a significant discrepancy in results between the homogenous analytical model and the finite element analysis when the elastic constant of the two materials do not match, and this becomes more significant as the layer size scale is reduced. We have compared the results obtained from our modelling scheme with the previous model, and with independently obtained finite element simulation results of the same material design scheme. We conclude that our assumption yields an accurate representation of the damage tolerance phenomenon observed in such layered composites. The results compare favourably with those from the previous analytical model, justifying our assumptions. This result also demonstrates that material inhomogeneity at small size scales can be successfully incorporated into a material behaviour model by treating these inhomogeneities as if they were distributed uniformly when observed at larger size scales. Of course, in our case the scheme works particularly well because of the geometrical arrangement of material inhomogeneity, which lends itself well to treatment as an elasticity problem with far field stresses.

The modelling strategy presented here represents an important step forward towards the optimization of geometrical parameters for achieving the highest possible threshold stress in a bimaterial laminate geometry in a given material system. It allows a straightforward method of predicting the variation in the damage tolerance obtained as the geometrical properties of the composite are modified. We have applied our model to optimizing the geometrical parameters for a silicon–silicon oxide composite with utility as a robust material for MEMS applications. Residual stress layer widths for this material lie in the micrometre and sub-micrometre range. The nature of the fabrication process at these layer widths is such that it allows extremely

fine control (<5 nm) over the final widths of each layer. Moreover, the final layer widths to be obtained are picked right at the beginning of the fabrication process, and the process parameters themselves are affected by the widths to be obtained. This analysis is therefore extremely important towards process planning. Optimization of the layer width ratio shows that even at nanometre scale compressive layer widths, a tensile/compressive layer width ratio between 0.5 and 1 can achieve the optimal threshold strength. In addition, at these size scales, the difference between the peak for threshold strength is relatively sharp, and a difference of ∼100 MPa threshold strength may be obtained by optimizing the layer width ratio as opposed to picking a width ratio based on other considerations such as ease of fabrication. The results obtained from our calculations enable us to pursue our goal of obtaining the highest possible threshold strength from our silicon–silicon oxide material system, even with very thin compressive layers. Moreover, it is clear that while the homogeneous model can perhaps be employed without lack of accuracy in predicting the behaviour of a laminate of this nature at conventional size scales, it becomes inadequate when designing nanometre scale composites that may be useful as MEMS structural materials.

Acknowledgments

This research was supported by funds provided by the Kavli Chair in MEMS technology in the Mechanical and Environmental Engineering department at the University of California, Santa Barbara, and by the National Science Foundation under award number CMS-0000142 and by DARPA-MTO contract DABT63-95-c0121. We thank Robert M McMeeking, Fred Lange, Masa Rao and Alexei Romanov for useful discussions.

References

[1] Rao M P, Sanchez-Herencia A J, Beltz G E, McMeeking R M and Lange F F 1999 *Science* **286** 102–5
[2] Rao M P and Lange F F 2002 *J. Am. Ceram. Soc.* **85** 1222–28
[3] Paranjpye A, MacDonald N C and Beltz G E 2004 A nanoscale composite material for enhanced damage tolerance in MEMS applications *NSTI Nanotechnology Conf. and Trade Show (Boston, 2004)* vol 1, p 363–6
[4] Hillman C, Suo Z G and Lange F F 1996 *J. Am. Ceram. Soc.* **79** 2127–33
[5] McMeeking R M and Hbaieb K 1999 *Z. Metallk.* **90** 1031–6
[6] Hbaieb K and McMeeking R M 2002 *Mech. Mater.* **34** 755–72
[7] Tada H, Paris P C, Irwin G R and Corporation D R 1985 *The Stress Analysis of Cracks Handbook*, 2nd edn (St Louis: Paris Productions)
[8] Zak A R and Williams M L 1963 *J. Appl. Mech.-Trans. ASME* **30** 142–3
[9] He M Y and Hutchinson J W 1989 *Int. J. Solids Struct.* **25** 1053–67
[10] Beuth J L 1992 *Int. J. Solids Struct.* **29** 1657–75